HAL
open science

Dynamics Consensus between Centroidal and Whole-Body Models for Locomotion of Legged Robots

Rohan Budhiraja, Justin Carpentier, Nicolas Mansard

▶ **To cite this version:**

Rohan Budhiraja, Justin Carpentier, Nicolas Mansard. Dynamics Consensus between Centroidal and Whole-Body Models for Locomotion of Legged Robots. 2018. hal-01875031v1

HAL Id: hal-01875031

https://laas.hal.science/hal-01875031v1

Preprint submitted on 16 Sep 2018 (v1), last revised 2 Apr 2019 (v3)

HAL is a multi-disciplinary open access archive for the deposit and dissemination of scientific research documents, whether they are published or not. The documents may come from teaching and research institutions in France or abroad, or from public or private research centers.

L'archive ouverte pluridisciplinaire **HAL**, est destinée au dépôt et à la diffusion de documents scientifiques de niveau recherche, publiés ou non, émanant des établissements d'enseignement et de recherche français ou étrangers, des laboratoires publics ou privés.

Dynamics Consensus between Centroidal and Whole-Body Models for Locomotion of Legged Robots

Rohan Budhiraja, Justin Carpentier and Nicolas Mansard

***Abstract*— It is nowadays well-established that locomotion can be written as a large and complex optimal control problem. Yet, current knowledge in numerical solver fails to directly solve it. A common approach is to cut the dimensionality by relying on reduced models (inverted pendulum, capture points, centroidal). However it is difficult both to account for whole-body constraints at the reduced level and also to define what is an acceptable trade-off at the whole-body level between tracking the reduced solution or searching for a new one. The main contribution of this paper is to introduce a rigorous mathematical framework based on the Alternating Direction Method of Multipliers, to enforce the consensus between the centroidal state dynamics at reduced and whole-body level. We propose an exact splitting of the whole-body optimal control problem between the centroidal dynamics (under-actuation) and the manipulator dynamics (full actuation), corresponding to a re-arrangement of the equations already stated in previous works. We then describe with details how alternating descent is a good solution to implement an effective locomotion solver. We validate this approach in simulation with walking experiments on the HRP-2 robot.**

I. Introduction

A. Motivation

Trajectory optimization for generating dynamically feasible motions remains a complex and challenging problem for legged robots. The main difficulty arises from a complex non-convex dynamics and the high dimensionality of the problem in which numerous Degrees of Freedom (DoF) must be coordinated together to create a feasible and optimal solution.

Most of the recent efforts in the robotics community have been focused on reducing the dimensionality and the complexity of the problem by relying on reduced models (e.g. table-cart [1], capture point [2] etc). One such approach which has recently gained in popularity is based on computing first the reference trajectory for the centroidal dynamics [3] of the robot, and then using this trajectory to generate a whole-body motion which is dynamically consistent [4], [5], [6]. It is easy to understand the reason behind this popularity: the problem is divided into two consecutive subproblems of smaller dimensions than the original problem, and thus are individually easier to solve. In addition, and contrary to other approaches, centroidal dynamics is exact projection of the full dynamics, which does not rely on any assumptions (like the constant altitude of the Center of Mass (CoM) for the table-cart model)

However, to guaranty the effectiveness of this splitting and to ensure that the two subproblems do not produce divergent and incoherent solutions at the global level, additional constraints must be enforced. These additional constraints can then be represented either explicitly, for example by using the whole-body kinematics in the centroidal optimization problem [4], or implicitly by relying on proxy constraints [7] to encode the full body behavior. Although adding explicit constraints in the subproblem is computationally expensive, proxy constraints on the CoM have shown good results [7] in multiple scenarios. However, it is difficult to define proxy constraints for all the centroidal quantities, especially the Angular Momentum (AM).

An alternative approach introduced in [8] and then exploited in [9], consists of alternating between the reduced and the whole-body problems in a recursive way. In [8] for instance, the CoM and AM trajectories in the reduced dynamics problem must track the output CoM and AM trajectories resulting from the whole-body dynamics and vice-versa, in order to enforce the feasibility between the two subproblems.

Other approaches have been introduced which compensate for the variations in AM [10], [11]. While they have produced good results, they are not yet able to generate additional momentum based on demands by the whole-body optimizer to enable very dynamic movements, as required (for instance) for fast locomotion [12], where the necessity of angular-momentum (AM) variations is imposed by the motion of the swing leg.

B. Overview of the contribution

In this paper, we aim to tackle the problem of generating consistent and coherent momentum (CoM and AM) at both centroidal and whole-body levels. We claim that given the efficacy of currently available solvers to solve the centroidal dynamics problem [13], a feedback from the whole-body dynamics solver [14] towards the centroidal problem will improve the consistency of the global locomotion solution within a few (perhaps only one) iterations.

However, mathematical rigor should not be avoided in the face of a good heuristic. None of the aforementioned methods *ensure* good convergence properties of the 2 subproblems to a common and same solution (a consensus), notably for the angular momentum. Rather, they rely on the ability of the individual solvers to produce consistent solutions without properly considering the global structure of the problem.

Our main contribution is to introduce a well-posed mathematical formulation that properly enforces the consensus between the two subproblems. Rather than

The Authors are with CNRS, LAAS, 7 Avenue du Colonel Roche, Toulouse, France. *email*: rohan.budhiraja@laas.fr

giving the solution of the whole-body problem directly to the centroidal optimizer as done by [8], we rely on the Alternating Direction Method of Multipliers (ADMM) technique to handle this feedback communication.

ADMM is an old but well established method for solving convex problems in which the objective is separable into two mutually exclusive cost functions along a set of problem variables. While the method has been around for decades, it was recently reintroduced [15] to solve large scale distributed optimization problems subject to constraints. ADMM provides a feedback to the subproblems in the form of the sum of the residues on the constraints, and in that fashion, it behaves similar to an integral controller. For example, the feedback property has been exploited in [16] to alternate between trajectory and policy optimization.

We find that the robustness and simplicity of this technique makes it an ideal candidate for solving the global optimization problem of locomotion as well. However, a clean splitting of quantities involved in the locomotion problem is required to make the individual subproblems really independent one from each other.

C. Outline of the paper

In Section II, we recall the optimal control problem (OCP) dedicated for locomotion and exhibit a complete splitting between centroidal and Lagrangian dynamics. We make obvious the cost implied by solving both subproblems without consensus. In Section III, we detail how ADMM can be exploited to solve the complete OCP by alternatively solving the two subproblems. We gather the details of implementation in Section IV, used to obtained experimental results on the HRP-2 robot in Section V.

II. The Locomotion Problem

A. Natural splitting of the robot dynamics

If we consider a legged robot dotted with n DoF, its whole-body dynamics is represented by the Lagrangian equations of motion:

$$\begin{bmatrix}\mathbf{H}_u\\ \mathbf{H}_a\end{bmatrix}\ddot{\mathbf{q}}+\begin{bmatrix}\mathbf{b}_u\\ \mathbf{b}_a\end{bmatrix}=\begin{bmatrix}\boldsymbol{g}_u\\ \boldsymbol{g}_a\end{bmatrix}+\begin{bmatrix}\mathbf{0}_6\\ \boldsymbol{\tau}\end{bmatrix}+\sum_{k=1}^{K}\begin{bmatrix}\mathbf{J}_{k,u}^\top\\ \mathbf{J}_{k,a}^\top\end{bmatrix}\boldsymbol{\lambda}_k \tag{1}$$

where $\mathbf{H}$ denotes the joint space inertia matrix, $\mathbf{b}$ encompasses the nonlinear effects, $\boldsymbol{g}$ corresponds to the generalized gravity vector, and $\mathbf{J}_k$ is the geometric Jacobian for contact k and λ_k is the vector of contact forces at contact point k. This dynamics can be split into two distinct parts: the 6 first rows correspond to the so-called under-actuated dynamics (denoted by the subscript u) while the n following rows correspond to the actuated dynamics (denoted by the subscript a).

The under-actuated dynamics of (1) is also known as the centroidal dynamics of the robot. It is governed by the Newton-Euler equations of motion which link the variations of the linear momentum and AM to the contact forces:

$$\begin{aligned} m\,\ddot{\mathbf{c}} &= \textstyle\sum_k \boldsymbol{\lambda}_k + m\,\mathbf{g}\\ \dot{\boldsymbol{L}} &= \textstyle\sum_k (\boldsymbol{p}_k-\mathbf{c})\times\boldsymbol{\lambda}_k \end{aligned} \tag{2}$$

where $\boldsymbol{p}_k$ is the position of the kth contact point, the operator $\times$ denotes the cross product, m is the total mass of the system, $\mathbf{c},\dot{\mathbf{c}},\ddot{\mathbf{c}}$ are the center of mass position, velocity and acceleration vectors and $\boldsymbol{L},\dot{\boldsymbol{L}}$ are the AM vector and its time derivative.

Thus, a natural splitting appears between two sets of state and control variables, namely:

- the centroidal set called $\mathbf{d}_c$ with state $\mathbf{x}_c=(\mathbf{c},\dot{\mathbf{c}},\boldsymbol{L})$ and control $\mathbf{u}_c=(\boldsymbol{\lambda}_1,\boldsymbol{\lambda}_2,\dots,\boldsymbol{\lambda}_k)$;
- the Lagrangian set named $\mathbf{d}_l$ with state $\mathbf{x}_l=(\mathbf{q},\dot{\mathbf{q}})$ and control $\mathbf{u}_l=\boldsymbol{\tau}$.

B. The global Optimal Control Problem for locomotion

Consider the scenario where the set of contact phases $\mathbf{S}$ and their corresponding contact timings Δt_s are already defined. Further, if we assume that the actuators are capable enough to provide sufficient torque (which is true for current generation of robots), it is possible to split the global motion planning Optimal Control Problem (OCP) between two states of the robot ($\boldsymbol{x}_{init}$, $\boldsymbol{x}_{final}$) into two hierarchical stages, which successively solve for $\underline{\mathbf{d}}_c$ and $\underline{\mathbf{d}}_l$. However, such an approach mandates that the solution of the first OCP is feasible for the second OCP. The kinematic feasibility condition between $\mathbf{q}$ and $\mathbf{c}$ has been explored [7] previously by our team.

The motion planning OCP, governed by the dynamics defined by (1) and (2), and the feasibility criteria given in [7] is given by[1]:

$$\begin{aligned}
\underset{\underline{\mathbf{d}}_c,\underline{\mathbf{d}}_l}{\text{minimize}}\quad & \sum_{s=1}^{S}\int_{t_s}^{t_s+\Delta t_s}\ell_s^c(\mathbf{d}_c)\,dt+\sum_{s=1}^{S}\int_{t_s}^{t_s+\Delta t_s}\ell_s^l(\mathbf{d}_l)\,dt && \text{(3a)}\\
\text{subject to}\quad & \forall t\quad \mathbf{c}=CoM(\mathbf{q}) && \text{(3b)}\\
& \forall t\quad \begin{bmatrix}m\dot{\mathbf{c}}\\ \boldsymbol{L}\end{bmatrix}=\boldsymbol{A}_g(\mathbf{q})\,\dot{\mathbf{q}} && \text{(3c)}\\
& \forall t\quad \boldsymbol{\lambda}=g_\lambda(\mathbf{q},\dot{\mathbf{q}},\boldsymbol{\tau}) && \text{(3d)}\\
& \forall t\quad \boldsymbol{\lambda}\in\mathcal{K} && \text{(3e)}\\
& \forall t\quad g_\lambda(\mathbf{q},\dot{\mathbf{q}},\boldsymbol{\tau})\in\mathcal{K} && \text{(3f)}\\
& \forall t\quad \dot{\mathbf{x}}_c=f_c(\mathbf{d}_c) && \text{(3g)}\\
& \forall t\quad \dot{\mathbf{x}}_l=f_l(\mathbf{d}_l) && \text{(3h)}\\
& \mathbf{x}_c(0)\text{ is given},\mathbf{x}_c(T)\text{ is viable} && \text{(3i)}\\
& \mathbf{x}_l(0)\text{ is given},\mathbf{x}_l(T)\text{ is viable} && \text{(3j)}
\end{aligned}$$

where s is the index of the contact phase, t_s is the start time of the contact phase s. ℓ_s^c and ℓ_s^l are local cost functions related to the phase. $\boldsymbol{A}_g$ is the so-called centroidal momentum matrix [3], and CoM maps the current joint configuration $\mathbf{q}$ to the center of mass position. g_λ is the mapping between the whole-body dynamics and contact forces, and may be dependent [14] or independent [17] from $\boldsymbol{\tau}$, depending on the choice of contact model.

Most of constraints and the two cost terms only depend on one of the two groups of variables $\underline{\mathbf{d}}_c,\underline{\mathbf{d}}_l$: $\ell_s^c(\mathbf{d}_c)$,

[1]Note that for all variables, underlines denote a trajectory of the variable over time. Similarly he dependency to the time variable is kept implicit i.e. $\forall t$ $\mathbf{c}$ is preferred to $\forall t$ $\mathbf{c}(t)$.

(3e), (3g) and (3i) define a problem over the centroidal dynamics ; $\ell_s^c(\mathbf{d}_l)$, (3f), (3h) and (3j) define a problem over the Lagrangian dynamics. The two groups are coupled by constraints (3b), (3c) and (3d). One way to solve the two problems independently is to replace these three coupling constraints by some proxy constraint, i.e. reformulation which enforces the existence of a global consensus solution acceptable by both subproblems. In [7], we have proposed to learn such a proxy constraints for the centroidal optimization. In the experiments of this paper, we will use again this learned proxy in the initial step of our algorithms.

Constraints (3e) and (3f) are redundant (i.e. (3e) and (3d) implies (3f)). Both of these constraints impose non-slippage conditions on the contact forces. (3e) and (3g) enforce consistent centroidal dynamics (2), while (3f) and (3h) enforce consistence of the Lagrangian dynamics (1) with respect to the contact model. We explicitly formulate both constraints to make the split evident. Similar remark holds for initial and terminal conditions (3i) and (3j). As terminal constraints are often difficult to formulate in practice, they should likely be replaced by stopping motion conditions (e.g. capturability) [18].

The near-perfect split has already been observed [8]. In this nice work, the observation was mostly used to justify the classical approach of separately solving each subproblem. Here we rather want to insist on the coupling and pave the way to the use of alternated descent.

C. Why should we alternate?

In a first implementation, it is often proposed to first compute the centroidal pattern and then track it by solving the Lagrangian dynamics. The most practical solution is likely to solve the first subproblem using additional reduction (e.g. the table-cart model with constant center of mass elevation). Then the whole-body movement is computed with an Inverse Kinematics (IK)/Inverse Dynamics (ID), which are theoretically equivalent to solving the Lagrangian part of (3) but with a void horizon $T = 0$. With such a simplification, it is almost always required that the AM trajectory output from the centroidal problem must be near perfectly tracked by the Lagrangian part. However, this is not possible. Although this assertion is known by many teams that already alternate by one way or the other on the two subproblems, we believe that it is not sufficiently documented and explain why alternating is important.

Momentum variations are caused by both, the forces exerted by the environment at the contact level, and by the motion of the limbs (also called "gesticulation" [12]). As the centroidal model does not account for the gesticulation, it is not possible to get the correct momentum when only considering it. Consider the example of the biped locomotion gait: an astronaut mimicking walk in deep space would rotate (pitch rotation) on the spot (same for a falling cat [12]). This is due to the movements of the limbs going forward when the leg is bent (short), and backward when the leg is stretched (long). As we are not rotating during locomotion, we can conclude that we exert some contact forces to counterbalance this rotation effect. Thus, these extra forces cannot be decided from the centroidal model alone. Consequently, perfectly tracking the momentum and the forces only by solving the centroidal model is impossible, and trying to approximately match the AM computed by the centroidal solver is a bad idea.

Moreover, it might be necessary to slow down or fasten the CoM (linear momentum) to avoid violating the force limits when excessive AM is generated by limb movements. Modifying the CoM in such a way is only possible if considering a preview horizon, i.e. not using an IK to compute the whole body.

A pragmatic solution is to compute the centroidal pattern by trying to match the AM that the limbs will generate. This implicitly suggests that we are not expecting to use the AM variations to improve the walk, but we are just trying to compensate for it. This is the standard implementation of the table-cart pattern generator, by adding a second stage of ZMP-CoM computation [10]. It has also been proposed to couple an IK with a centroidal solver [5]. In both cases, it has been experimentally observed that alternating twice is enough in practice. However, no theoretical guarantee has yet been provided. This is what we propose to do in the following Sec III

III. Alternating method for locomotion

In this section, we first review the ADMM technique. We then apply it on the global OCP for locomotion (3).

A. Alternating Direction Method of Multipliers

ADMM is a simple optimization technique to solve constrained problems of the form:

$$\begin{aligned} \underset{\boldsymbol{x},\boldsymbol{z}}{\text{minimize}} \quad & l_1(\boldsymbol{x}) + l_2(\boldsymbol{z}) \\ \text{subject to} \quad & A\boldsymbol{x} + B\boldsymbol{z} = \boldsymbol{c} \end{aligned} \tag{4}$$

where the cost function is composed of two separable objectives $l_1(\boldsymbol{x})$ and $l_2(\boldsymbol{z})$. The main idea behind ADMM is to exploit this splitting between cost terms in a recursive manner, allowing to solve simpler problems than the original one. This precise point can be highlighted by writing the augmented Lagrangian associated with the constrained optimization problem (4):

$$\begin{aligned} \mathcal{L}_\rho(\boldsymbol{x},\boldsymbol{z},\boldsymbol{y}) = l_1(\boldsymbol{x}) + l_2(\boldsymbol{z}) + \boldsymbol{y}^T(A\boldsymbol{x} + B\boldsymbol{z} - \boldsymbol{c}) \\ + \frac{\rho}{2}\left\|A\boldsymbol{x} + B\boldsymbol{z} - \boldsymbol{c}\right\|_2^2 \end{aligned} \tag{5}$$

where $\boldsymbol{y}$ is the vector of dual variables associated with the constraint $A\boldsymbol{x} + B\boldsymbol{z} = \boldsymbol{c}$ and $\rho > 0$ is the penalty parameter which penalizes the violations of this constraint. The solution is then found by the following steps recursions[2]:

$$\boldsymbol{x}^{k+1} = \underset{\boldsymbol{x}}{\operatorname{argmin}}\, \mathcal{L}_\rho(\boldsymbol{x}, \boldsymbol{z}^k, \boldsymbol{y}^k) \tag{6a}$$

$$\boldsymbol{z}^{k+1} = \underset{\boldsymbol{z}}{\operatorname{argmin}}\, \mathcal{L}_\rho(\boldsymbol{x}^{k+1}, \boldsymbol{z}, \boldsymbol{y}^k) \tag{6b}$$

$$\boldsymbol{y}^{k+1} = \boldsymbol{y}^k + \rho(A\boldsymbol{x} + B\boldsymbol{z} - \boldsymbol{c}) \tag{6c}$$

[2]Throughout the paper, superscripts are used to refer to the current iteration of the solver

Problem (6a) and (6b) are simply minimization over l_1 and l_2 respectively (with some additional quadratic terms which are solvable with the current generation of solvers). It is also worth noticing that the dual variables $\boldsymbol{y}$, through the update (6c) act as an integral term by collecting the residues on the consensus between the two subproblems, and forces the residual to converge to 0 along the iterations.

B. ADMM for locomotion rational

ADMM provides a way for us to exploit the splitting of dynamic variables exposed in Sec II-B, and defines a mathematical framework to feedback and optimize the AM variable inside the centroidal OCP.

OCP (3) does not match exactly the pattern of (4): (3) has 3 nonlinear coupling constraints and additional decoupled constraints. For the 3 semi-infinite (i.e. defined $\forall t$) coupling constraints, we have to introduce 3 multipliers functions of time. For the additional decoupled constraints, we handle them in the two solvers of each subproblems. It would only burden the equations to mention them in the alternated scheme. Let us remember that the partial solutions $\underline{\mathbf{d}}_c$ and $\underline{\mathbf{d}}_l$ of each subproblems should respect these additional constraints. In this section, we explain the alternating algorithm with the hypothesis that some oracles can be called to provide the optimum of the two subproblems. The next section will describe with more details which centroidal and whole-body solvers we used for the experiments.

Non-linearity is a theoretical issue and it makes the problem non-convex. Converge guarantee with ADMM are yet only obtained for convex problem. Yet we at least know that the linearization of (3) will converge. On-going theoretical works try to show that local convergence can be obtain in non-convex cases. Moreover, in practice, ADMM is often used, with good empirical results, for non-convex problems.

C. Application of ADMM to the locomotion problem

Let us associate with each coupling constraint a residual function:

$$\forall t \quad \boldsymbol{r}_c(\mathbf{c}, \mathbf{q}) = \mathbf{c} - CoM(\mathbf{q}) \tag{7a}$$

$$\forall t \quad \boldsymbol{r}_m(\dot{\mathbf{c}}, \boldsymbol{L}, \mathbf{q}, \dot{\mathbf{q}}) = \begin{bmatrix} m\dot{\mathbf{c}} \\ \boldsymbol{L} \end{bmatrix} - \boldsymbol{A}_g(\mathbf{q})\,\dot{\mathbf{q}} \tag{7b}$$

$$\forall t \quad \boldsymbol{r}_\lambda(\lambda, \mathbf{q}, \dot{\mathbf{q}}, \tau) = \lambda - g_\lambda(\mathbf{q}, \dot{\mathbf{q}}, \tau) \tag{7c}$$

Residuals $\underline{\boldsymbol{r}}_c, \underline{\boldsymbol{r}}_m, \underline{\boldsymbol{r}}_g$ respectively corresponds to constraints (3b), (3c), (3d). We also respectively define $\underline{\boldsymbol{y}}_c, \underline{\boldsymbol{y}}_m, \underline{\boldsymbol{y}}_g$ as the multipliers corresponding to these 3 constraints.

We denote by $\underline{\boldsymbol{r}}$ the augmentation (i.e. sum of linear and quadratic penalization on the multipliers) of (3):

$$\underline{\boldsymbol{r}}(\underline{\mathbf{d}}_c, \underline{\mathbf{d}}_l, \underline{\boldsymbol{y}}) = \sum_{k=m,c,\lambda} \int_0^{T_f} \boldsymbol{y}_k^T(t)\boldsymbol{r}_k(t) + \frac{\rho_k(t)}{2}\left\|\boldsymbol{r}_k(t)\right\|_2^2 \, dt \tag{8}$$

We can now separate the augmented Lagrangian of the global OCP into centroidal and full body parts:

$$\begin{aligned} \mathcal{L}_\rho^c(\underline{\mathbf{d}}_c, \underline{\mathbf{d}}_l, \underline{\boldsymbol{y}}) &= \sum_{s=1}^{S} \int_{t_s}^{t_s+\Delta t_s} \ell_s^c(\mathbf{d}_c)\, dt + \underline{\boldsymbol{r}} \\ \mathcal{L}_\rho^l(\underline{\mathbf{d}}_c, \underline{\mathbf{d}}_l, \underline{\boldsymbol{y}}) &= \sum_{s=1}^{S} \int_{t_s}^{t_s+\Delta t_s} \ell_s^l(\mathbf{d}_l)\, dt + \underline{\boldsymbol{r}} \end{aligned} \tag{9}$$

where $\boldsymbol{y}$ is the stack of the 3 multipliers. Note that the multipliers are trajectories of vectors, while $\rho_c, \rho_m, \rho_\lambda$ are trajectories of scalars.

Using the definition of ADMM from Sec III-A, the global OCP can thus be solved by the following iterations:

$$\begin{aligned} &\underline{\mathbf{d}}_c^{k+1} = \underset{\underline{\mathbf{d}}_c}{\operatorname{argmin}}\, \mathcal{L}_\rho^c(\underline{\mathbf{d}}_c, \underline{\mathbf{d}}_l^k, \underline{\boldsymbol{y}}^k) \text{ subject to } (3e), (3g), (3i) \\ &\underline{\mathbf{d}}_l^{k+1} = \underset{\underline{\mathbf{d}}_l}{\operatorname{argmin}}\, \mathcal{L}_\rho^l(\underline{\mathbf{d}}_c^{k+1}, \underline{\mathbf{d}}_l, \underline{\boldsymbol{y}}^k) \text{ subject to } (3f), (3h), (3j) \\ &\forall t \quad \boldsymbol{y}_c^{k+1} = \boldsymbol{y}_c^k + \rho_c(\mathbf{c}^{k+1} - CoM(\mathbf{q}^{k+1})) \\ &\forall t \quad \boldsymbol{y}_m^{k+1} = \boldsymbol{y}_m^k + \rho_m(\begin{bmatrix} m\dot{\mathbf{c}}^{k+1} \\ \boldsymbol{L}^{k+1} \end{bmatrix} - \boldsymbol{A}_g\left(\mathbf{q}^{k+1}\right)\dot{\mathbf{q}}^{k+1}) \\ &\forall t \quad \boldsymbol{y}_\lambda^{k+1} = \boldsymbol{y}_\lambda^k + \rho_\lambda(\lambda^{k+1} - g_\lambda(\mathbf{q}^{k+1}, \dot{\mathbf{q}}^{k+1}, \tau^{k+1})) \end{aligned} \tag{10}$$

IV. Alternating using dedicated solvers

In this section, we describe the practical details of our implementation, enabling us to simply add the alternating descent on top of our existing frameworks for solving centroidal and whole-body dynamics OCP, with only a minor additional cost in terms of development.

A. The locomotion pipeline

Our locomotion pipeline called Loco3d is described in [19]. It is composed of three main stages:

1) The Contact Sequence Generator: It is a randomized motion planner [20], which ensures the feasibility of the sequence at the kinematic level, with real-time performances;

2) The Centroidal Optimizer: It solves the trajectory optimization problem over the centroidal dynamics using feasibility measures to enforce the kinematic feasibility of the solution with respect to the whole-body problems. It relies on MUSCOD-II [21], an optimal control framework which implements an efficient multiple-shooting algorithm particularly suited for the multiple contact phases of the locomotion problem;

3) The Whole-Body Optimizer: We use a new iterative Differential Dynamic Programming (DDP) solver [14] which accounts for the contact constraints in the dynamics of the problem.

B. On the advantages of scaling the dual variables

Scaling the dual variables through $\boldsymbol{z} = \frac{\boldsymbol{y}}{\rho}$ is more convenient to implement as it combines under a single norm minimization both the linear and quadratic terms in the augmented Lagrangian (9). The subproblems are then reduced to simply minimize the residual squared norm of the constraints linking the two problems [15].

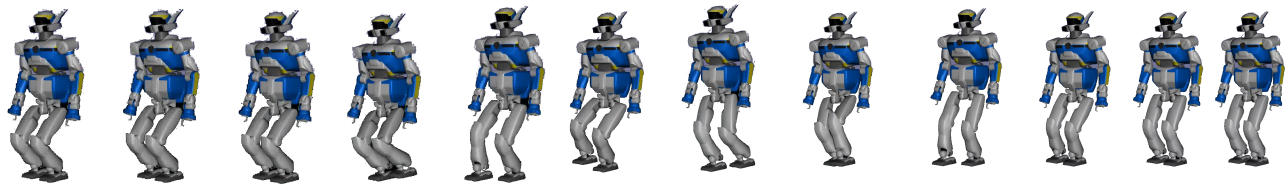

Fig. 1: Walking sequence generated for HRP-2 robot using the proposed ADMM solver.

C. The ADMM solver for locomotion

By using $\underline{z}$, we can simplify the notation further by collecting the constraints (3b), (3c) and (3d) into a single quantity. For that aim, let us define Φ_c to contain the elements $(\boldsymbol{c}, m\dot{\mathbf{c}}, \boldsymbol{L}$ and $\boldsymbol{\lambda})$. Similarly, let us define Φ_l to contain the mappings $(CoM(\mathbf{q}), \boldsymbol{A}_g(\mathbf{q})\,\dot{\mathbf{q}}$ and $g_\lambda(\mathbf{q}, \dot{\mathbf{q}}, \boldsymbol{\tau}))$. Let us define addition/subtraction operations on Φ to be the addition/subtraction on its corresponding elements and a function $DMap$ which maps the centroidal($\mathbf{d}_c$) and whole-body($\mathbf{d}_l$) variables onto these elements. The iterations (10) can be then written equivalently as Algorithm 1. In Algorithm 1, the first input to the solvers is the solution of the previous iteration (as a warm start), and the second input is the reference to be tracked for the augmented Lagrangian quadratic costs.

Algorithm 1: ADMM solver for locomotion

Data: $\underline{\mathbf{d}}_c^0, \underline{\mathbf{d}}_l^0$

$\underline{\mathbf{d}}_c \leftarrow \underline{\mathbf{d}}_c^0, \qquad \underline{\mathbf{d}}_l \leftarrow \underline{\mathbf{d}}_l^0;$

$\underline{\Phi}_c \leftarrow DMap(\underline{\mathbf{d}}_c), \quad \underline{\Phi}_l \leftarrow DMap(\underline{\mathbf{d}}_l);$

$\underline{\Phi}_d \leftarrow \underline{\Phi}_c - \underline{\Phi}_l;$

repeat

  $\underline{\mathbf{d}}_c, \underline{\Phi}_c \leftarrow CentroidalSolver(\underline{\mathbf{d}}_c, \underline{\Phi}_l - \underline{\Phi}_d);$

  $\underline{\mathbf{d}}_l, \underline{\Phi}_l \leftarrow WholebodySolver(\underline{\mathbf{d}}_l, \underline{\Phi}_c + \underline{\Phi}_d);$

  $\underline{\Phi}_d \leftarrow \underline{\Phi}_d + \underline{\Phi}_c - \underline{\Phi}_l;$

until *convergence*;

$\underline{\mathbf{d}}_c^* \leftarrow \underline{\mathbf{d}}_c, \qquad \underline{\mathbf{d}}_l^* \leftarrow \underline{\mathbf{d}}_l;$

Result: $\underline{\mathbf{d}}_c^*, \underline{\mathbf{d}}_l^*$

D. Initializing the dual variables

Many of the currently available centroidal and whole-body dynamics solvers are tailored for producing solutions which are almost always mutually solvable [8] [22] [14]. As a result, with this assumption of mutual solvability, a simple feedback from the whole-body solver to the centroidal solver generates acceptable result within the second iteration [8]. On the other hand, since ADMM transmits the residual of the two subproblems and not the output, an *uninitialized* ADMM solver would overshoot and only promise convergence from the third iteration, as we later see in Sec V. There is indeed a minimum number of iterations to synchronize the two subproblems.

However, this extra iteration of the solver could be avoided by setting the dual after the first iteration as $\underline{\Phi}_d^1 \leftarrow \underline{\Phi}_c^1$. This change makes the feedback from the first iteration to be equal to the output, and the knowledge of individual solvers can then be exploited to converge within two iterations. Indeed, the second iteration of the ADMM solver then becomes equivalent to [8], and would provide similar results without affecting convergence. While not used in this paper, this trick needs to be evaluated further.

E. Key observations for the centroidal solver

In the centroidal OCP, there is a redundancy in the state. The state $\mathbf{c}, \dot{\mathbf{c}}, \boldsymbol{L}$ has a dimension of 9, while the control can be represented in a dimension 6 (with a centroidal wrench acting on the center of mass). This redundancy is usually suppressed by predefining or regularizing $\boldsymbol{L}$ [7], and solving for the rest. The same principle can be exploited in the present case, by predefining $\underline{\boldsymbol{L}}^{k+1}$ to be equal to the AM part of $\underline{\Phi}_l^k - \underline{\Phi}_d^k$ and solving the centroidal step only for $\underline{\mathbf{c}}^{k+1}, \underline{\dot{\mathbf{c}}}^{k+1}, \underline{\lambda}^{k+1}$. This method ensures that the AM is always consistent with the full body dynamics.

As a result, angular part of $\boldsymbol{r}_m$ is always zero after the centroidal step of (10). Equivalently, variations in the AM part of $\underline{\Phi}_d^{k+1}$ are only dependent on the variations in the AM part of $\underline{\Phi}_l^{k+1}$ ($\boldsymbol{L}$ is given as a feedback from the full-body OCP to centroidal OCP via $\boldsymbol{r}_m$)

F. Key observations for whole-body solver

During the full-body step of (10), the knowledge of λ^{k+1} from the centroidal step can be exploited to ensure that the Constraint (3f) is never violated. In the full-body step (by the mapping g_λ) λ is dependent on $\mathbf{q}, \dot{\mathbf{q}}, \tau$. A predefined λ_{ref}^{k+1} provides a good tracking reference for the contact forces. With a good tracking, Constraint (3f) can be relaxed. An implementation of the full-body step with rigid contacts which exploits such a reference tracking is proposed in [14]. Note that in [14] $\mathbf{c}$ and λ were being tracked in the full-body OCP, while in the present formulation they are updated during the dual ascent.

V. Experimental results

In this section, we validate and highlight the efficiency of the proposed approach in simulation. For that purpose, we study the convergence properties of our solver on a simplified version of the humanoid robot HRP-2 only composed of its lower limbs. We generate a walking motion composed of 3 steps of 40 cm step length, depicted in Fig. 1.

A. Cost functions

1) The centroidal cost function:: for the first iteration of the centroidal solver, we minimize the log barrier on the feasibility measure of the CoM [7], and we regularize the CoM velocity (weight: 10) and contact forces (weight:10^{-4} for linear and 10^{-2} for angular) with quadratic costs. For

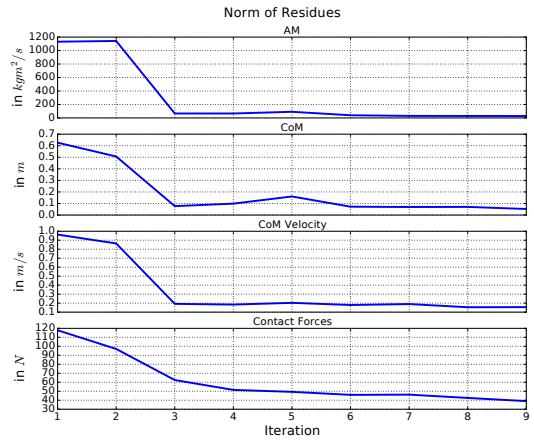

Fig. 2: Evolution of the total norm of the constraint residual along the iterations of the ADMM solver.

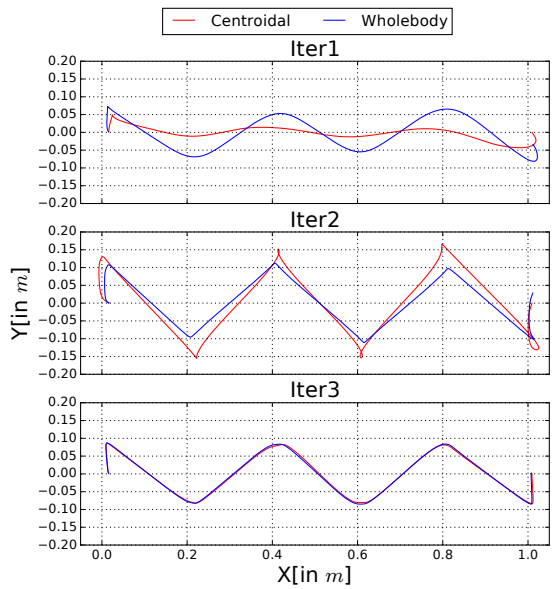

Fig. 3: CoM trajectory in the XY plane for the first three iterations of the ADMM solver.

subsequent iterations, we solely minimize the dual terms with $\rho_c = 1.0, \rho_m = 10^{-2}$ and $\rho_\lambda = 10^{-4}$.

2) The whole-body cost function:: For the whole-body solver, we use only quadratic costs to regularize the posture (weight: 10^{-6}) and the free-flyer orientation (weight: 20) in addition to the augmented Lagrangian terms.

B. Convergence analysis

We stopped the alternating resolution after only 10 iterations of the solver described in Algorithm 1. While 3 iterations were sufficient to compute a feasible motion in simulation, we show here the continuing convergence. As shown in Fig. 2, the total residuals of the matching constraints decrease rapidly over the first three iterations and more slowly after. This really means that the two problem are able to find a consensus in very few iterations. This behavior

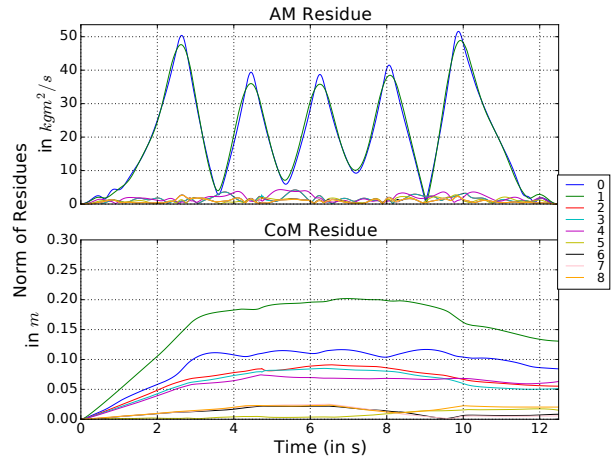

Fig. 4: Residue between the centroidal and whole-body trajectory of AM and CoM over the iterations.

is also well depicted in Fig. 3, where one can observe the CoM trajectories of both centroidal and whole-body subproblems. Already at iteration 3, the two trajectories match almost perfectly.

The mismatching of CoM and AM quantities is also reflected in Fig. 4. The two first iterations show a large mismatch between the centroidal and the whole-body problems, but the residual decreases rapidly towards the value 0. This phenomena can be explained by the delay induced by the ADMM approach: the solver overshoots and then builds and *maintains* a consensus between the two subproblems as discussed in Sec IV-D.

VI. Conclusion and Future Work

In this paper, we have introduced a systematic approach to build a consensus on the dynamics constraints between the centroidal and whole-body optimization problems. Based on previous observation between the nice articulation between under-actuated and actuated dynamics of legged robots, we have given a mathematical framework to separate the two problems, and proposed a solution which iterates between the two subproblems and maintains consensus in the solutions. Finally, we demonstrate with a walking sequence on HRP-2 the performance of the solver.

While some heuristics are available allowing similar behaviors, the ADMM solver encompasses the dynamics constraints within the framework of the solver itself. In this way, the current method deals with not only individual and separated subproblems, but tackles the global problem defined in (3). To the best of our knowledge, this is the first time that a consensus between centroidal and Lagrangian dynamic solvers is obtained based on theoretical grounding.

However, even if this solver currently solves the full-body dynamics problem, it assumes a dependence on the upstream contact planner to provide feasible contact planning. Thus, we need to ensure a similar consistency between the upstream contact planner and the full body optimizer as well. This is a future avenue of research for the community.

REFERENCES

[1] S. Kajita, F. Kanehiro, K. Kaneko, K. Yokoi, and H. Hirukawa, "The 3D linear inverted pendulum mode: a simple modeling for a biped walking pattern generation," in *IEEE International Conference on Intelligent Robots and Systems (IROS)*, 2001.

[2] J. Pratt, J. Carff, S. Drakunov, and A. Goswami, "Capture point: A step toward humanoid push recovery," in *Humanoid Robots, 2006 6th IEEE-RAS International Conference on*. IEEE, 2006, pp. 200–207.

[3] D. E. Orin, A. Goswami, and S.-H. Lee, "Centroidal dynamics of a humanoid robot," *Autonomous Robots*, vol. 35, no. 2-3, pp. 161–176, 2013.

[4] H. Dai, A. Valenzuela, and R. Tedrake, "Whole-body motion planning with centroidal dynamics and full kinematics," in *2014 IEEE-RAS International Conference on Humanoid Robots*. IEEE, nov 2014, pp. 295–302. [Online]. Available: http://ieeexplore.ieee.org/document/7041375/

[5] A. Herzog, N. Rotella, S. Schaal, and L. Righetti, "Trajectory generation for multi-contact momentum control," in *IEEE-RAS Int. Conf. on Humanoid Robotics (ICHR)*, 2015.

[6] J. Carpentier, S. Tonneau, M. Naveau, O. Stasse, and N. Mansard, "A versatile and efficient pattern generator for generalized legged locomotion," in *IEEE International Conference on Robotics and Automation (ICRA)*, 2016.

[7] J. Carpentier, R. Budhiraja, and N. Mansard, "Learning Feasibility Constraints for Multicontact Locomotion of Legged Robots," in *Robotics: Science and Systems (RSS)*, 2017.

[8] A. Herzog, S. Schaal, and L. Righetti, "Structured contact force optimization for kino-dynamic motion generation," in *IEEE International Conference on Intelligent Robots and Systems (IROS)*, 2016.

[9] B. Ponton, A. Herzog, S. Schaal, and L. Righetti, "A convex model of humanoid momentum dynamics for multi-contact motion generation," in *IEEE-RAS Int. Conf. on Humanoid Robotics (ICHR)*, 2016, pp. 842–849.

[10] S. Kajita, F. Kanehiro, K. Kaneko, K. Fujiwara, K. Harada, K. Yokoi, and H. Hirukawa, "Biped walking pattern generation by using preview control of zero-moment point," in *IEEE-RAS Int. Conf. on Robotics and Automation (ICRA)*, 2003.

[11] A. Herzog, N. Rotella, S. Mason, F. Grimminger, S. Schaal, and L. Righetti, "Momentum Control with Hierarchical Inverse Dynamics on a Torque-Controlled Humanoid," *Autonomous Robots*, 2016.

[12] P.-B. Wieber, "Holonomy and nonholonomy in the dynamics of articulated motion," in *Proceedings of the Ruperto Carola Symposium on Fast Motion in Biomechanics and Robotics*, 2005.

[13] J. Carpentier and N. Mansard, "Multi-contact locomotion of legged robots," *IEEE Transactions on Robotics (In Press)*, 2018.

[14] R. Budhiraja, J. Carpentier, C. Mastalli, and N. Mansard, "Differential dynamic programming for multi-phase rigid contact dynamics," 2018, submitted to IEEE International Conference on Humanoid Robots. [Online]. Available: https://hal.archives-ouvertes.fr/hal-01851596

[15] S. Boyd, N. Parikh, E. Chu, B. Peleato, and J. Eckstein, "Distributed Optimization and Statistical Learning via the Alternating Direction Method of Multipliers," *Foundations and Trends in Machine Learning*, vol. 3, no. 1, pp. 1–122, 2010.

[16] I. Mordatch and E. Todorov, "Combining the benefits of function approximation and trajectory optimization," in *Robotics: Science and Systems X*. Robotics: Science and Systems Foundation, jul 2014. [Online]. Available: http://www.roboticsproceedings.org/rss10/p52.pdf

[17] M. Neunert, M. Stauble, M. Giftthaler, C. D. Bellicoso, J. Carius, C. Gehring, M. Hutter, and J. Buchli, "Whole-Body Nonlinear Model Predictive Control Through Contacts for Quadrupeds," *IEEE Robotics and Automation Letters (RAL)*, 2018.

[18] P.-B. Wieber, "Viability and predictive control for safe locomotion," in *2008 IEEE/RSJ International Conference on Intelligent Robots and Systems*. IEEE, sep 2008, pp. 1103–1108.

[19] J. Carpentier, A. D. Prete, S. Tonneau, T. Flayols, F. Forget, A. Mifsud, K. Giraud, D. Atchuthan, P. Fernbach, R. Budhiraja, M. Geisert, J. Solà, O. Stasse, and N. Mansard, "Multi-contact Locomotion of Legged Robots in Complex Environments The Loco3D project," 2017, RSS Workshop on Challenges in Dynamic Legged Locomotion.

[20] S. Tonneau, A. D. Prete, J. Pettré, C. Park, D. Manocha, and N. Mansard, "An Efficient Acyclic Contact Planner for Multiped Robots," *IEEE Transactions on Robotics (TRO)*, 2018.

[21] D. Leineweber, I. Bauer, H. G. Bock, and J. P. Schlöder, "An efficient multiple shooting based reduced sqp strategy for large-scale dynamic process optimization. part 1: theoretical aspects," *Computers & Chemical Engineering*, 2003.

[22] J. Carpentier and N. Mansard, "Analytical Derivatives of Rigid Body Dynamics Algorithms," in *Robotics: Science and Systems (RSS)*, 2018.